Attention Microfiche User,

The original document from which this microfiche was made was found to contain some imperfection or imperfections that reduce full comprehension of some of the text despite the good technical quality of the microfiche itself. The imperfections may be:

- missing or illegible pages/figures
- wrong pagination
- poor overall printing quality, etc.

We normally refuse to microfiche such a document and request a replacement document (or pages) from the National INIS Centre concerned. However, our experience shows that many months pass before such documents are replaced. Sometimes the Centre is not able to supply a better copy or, in some cases, the pages that were supposed to be missing correspond to a wrong pagination only. We feel that it is better to proceed with distributing the microfiche made of these documents than to withhold them till the imperfections are removed. If the removals are subsequestly made then replacement microfiche can be issued. In line with this approach then, our specific practice for microfiching documents with imperfections is as follows:

1. A microfiche of an imperfect document will be marked with a special symbol (black circle) on the left of the title. This symbol will appear on all masters and copies of the document (1st fiche and trailer fiches) even if the imperfection is on one fiche of the report only.

2. If imperfection is not too general the reason will be specified on a sheet such as this, in the space below.

3. The microfiche will be considered as temporary, but sold at the normal price. Replacements, if they can be issued, will be available for purchase at the regular price.

4. A new document will be requested from the supplying Centre.

5. If the Centre can supply the necessary pages/document a new master fiche will be made to permit production of any replacement microfiche that may be requested.

The original document from which this microfiche has been prepared has these imperfections:

☒ missing pages/figures numbered: FIG: 7 is missing

☐ wrong pagination

☐ poor overall printing quality

☐ combinations of the above

☐ other

INIS Clearinghouse
IAEA
P. O. Box 100
A-1400, Vienna, Austria

Université Scientifique et Médicale de Grenoble

INSTITUT DES SCIENCES NUCLÉAIRES
DE GRENOBLE

53, avenue des Martyrs – GRENOBLE

ISN 82.07
March 1982

LEVEL STRUCTURE OF ^{60}Ni FROM THE ^{58}Ni(α,2pγ) REACTION

Tsan Ung Chan, C. Morand, F. Azgui, M. Agard[1], J.F. Brunndet, B. Chambon[2], A. Dauchy, D. Drain[2], A. Giorni and F. Glasser

[1]Institut des Sciences Exactes, Université de Constantine, Route d'Ain El Bey, Constantine, Algérie.

[2]Institut de Physique Nucléaire, 43 Boulevard du 11 Novembre, 69621 Villeurbanne, France.

Submitted to Physica Scripta

Laboratoire associé à l'Institut National de Physique Nucléaire et de Physique des Particules.

LEVEL STRUCTURE OF ^{60}Ni FROM THE ^{58}Ni(α,2pγ) REACTION

Tsan Ung Chan, C. Morand, F. Azgui, M. Agard[1], J.F. Bruandet
B. Chambon[2], A. Dauchy, D. Drain[2], A. Giorni and F. Glasser

Institut des Sciences Nucléaires (IN2P3-USMG)
53 Avenue des Martyrs - F 38026 Grenoble Cédex France

Institut des Sciences Nucléaires (USMG-IN2P3) 53 Av. des Martyrs - F 38026 Grenoble Cédex

ABSTRACT. The ^{60}Ni nucleus has been studied via the ^{58}Ni (α,2pγ) reaction at E_α = 32 MeV using in-beam γ spectroscopy techniques. High-spin states up to 10 MeV excitation have been established. Among the 5 branches depopulating the Yrast $J^\pi = 7^-$ state, has been found an E3 transition down to the 4^+ state. Comparison with direct reactions results leads to assign very probably the $[\nu f_{5/2}, \nu g_{9/2}]_{7^-}$ configuration to the $J^\pi = 7^-$ Yrast state at 5349 keV, suggesting then the $[\nu(p_{1/2}, p_{3/2}, f_{5/2})^2_{2^+} \times (\nu f_{5/2}, \nu g_{9/2})^2_{7^-}]_{9^-}$ configuration for the $J^\pi = 9^-$ Yrast state. Other high-spin states might be accounted for by the breaking of the ^{56}Ni core.

1) Institut des Sciences Exactes, Université de Constantine, Route d'Ain El Bey, Constantine, Algérie

2) Institut de Physique Nucléaire (UCB Lyon, IN2P3), 43 Bd du 11 Novembre 69621 Villeurbanne, France.

1) INTRODUCTION

A large amount of experimental and theoretical works have already been devoted to the study of the ^{60}Ni nucleus. The experimental data till 1979 have been compiled by Auble [1]. In contrast with low-spin states ($I \leq 5$) where informations are abondant, data on high-spin states ($J \geq 6$) are available only from gamma-ray spectroscopy. Many heavy-ion induced reactions [2,3] such as ^{46}Ti (^{16}O,2pγ), ^{50}Cr(^{12}C,2pγ) and ^{51}V(^{12}C,2np) have been used to populate high-spin states in ^{60}Ni. An intense γ ray cascade, referred as "C" cascade has been observed with Yrast spin sequence : 0^+, 2^+, 4^+, 6^+, 7^-, 9^-. Recently Kearns et al. [4] used ^{58}Fe(^{7}Li, p2nγ), ^{57}Fe(α,nγ), ^{56}Fe(^{6}Li,pnγ) and ^{52}Cr(^{10}B,pnγ) to get a more detailed scheme. In those reactions they observed the "C" cascade again, but no level above the 9^- state. Via direct reactions Hansen et al. [5,6] have studied two-proton transfer with the ^{58}Fe(^{16}O,^{14}C) ^{60}Ni reaction and α transfer with the ^{56}Fe(^{16}O,^{12}C)^{60}Ni reaction. Only levels up to $J^\pi = 4^+$ have been excited in these reactions.

Theoretical calculations concerning high-spin states are rather scarce. Rem Ray et al. [7] have reckoned negative parity states up to the $J^\pi = 7^-$ state at 5.30 MeV by means of the modified Tam-Dancoff approximation and assuming a ^{56}Ni inert core and the four extra-core neutrons occupying the $p_{3/2}$, $f_{5/2}$, $p_{1/2}$ and $g_{9/2}$ single particle orbitals. The shell model calculations of Koops et al. [8] kept the ^{56}Ni core but restricted the neutron orbitals to the $p_{3/2}$, $f_{5/2}$ and $p_{1/2}$ subshells so that they could only account for positive states up to $J^\pi = 6^+$.

Very recently, Rotbhare et al. [9] made shell-model calculations in the $(p_{1/2}, p_{3/2}, f_{5/2}, g_{9/2})$ space to explain the high-spin Yrast cascade in this nuclei. There is no doubt that the doubly magic nucleus ^{56}Ni with its first excited state $J^{\pi} = 2^{+}$ at 2700 keV forms an utterly inert core, and coupled to the 4 valence neutrons in the neighbouring orbitals $p_{3/2}$, $f_{5/2}$, $p_{1/2}$ and $g_{9/2}$ (their single particle energies are respectively 0 - 768 - 1112 and 3710 keV in ^{57}Ni) it provides a powerful picture to describe most of the lowest levels in ^{60}Ni. With regard to the 3.7 MeV energy of the $g_{9/2}$ orbital, only one neutron may be $g_{9/2}$, thus giving negative parity states with, for example, the following configuration $[g_{9/2}, f_{5/2}, (p_{3/2})^2_{0^+}]_{7^-}$, $[g_{9/2}, f_{5/2}, (p_{3/2}, p_{1/2})^2_{2^+}]_{9^-}$ $[g_{9/2}, (f_{5/2})^2, p_{3/2}]_{10^-}$ and so $J^{\pi} \leq 10^{-}$.

For positive parity states this picture only allows the maximum spin $J^{\pi} \leq 5^{+}$ with configurations $[(f_{5/2})^2_{4^+}, (p_{3/2})^2_{2^+}]$ for instance. Higher spin states would require in the $g_{9/2}$ shell 3 neutrons for negative parity states and 2 neutrons for positive parity states. With regard to the large energy gap for the $g_{9/2}$ shell, the breaking of the ^{56}Ni core could be a cheaper way to build higher spin states.

In this work, we show that α induced reaction, due to narrower excitations functions (few exit channels at a given incident energy) and little angular momentum required to populate the highest level spin, does in fact lead to more detailed results. Surprisingly, the high-spin states are in this case relatively more well fed than in H.I. induced reaction.

2) EXPERIMENTAL PROCEDURE

Using beams from the Grenoble cyclotron, isotopic ~ 1 mg/cm^2 ^{58}Ni targets, large volume Ge(Li) detectors (50-90 cm^3) with a typical resolution of 3 keV at $E_\gamma = 1.3$ MeV, the following measurements have been undertaken :

- yield functions of γ-rays : $E_\alpha = 23 - 40$ MeV
- angular distributions at $E_\alpha = 32$ MeV
- γ-γ coincidences at $E_\alpha = 32$ MeV
- lifetime measurements with DSAM at $E_\alpha = 32$ MeV

Fig. 1 shows a single γ-ray spectrum of ^{58}Ni + α at $E_\alpha = 32$ MeV. The main channels are $(\alpha,2p\gamma)^{60}$Ni, $(\alpha,pn\gamma)^{60}$Cu and $(\alpha,\alpha p\gamma)^{57}$Co (the intensity are respectively in the 6/3/1 ratios). An accurate calibration of high energy gamma is provided by intense gamma rays from the radioactivity of ^{60}Cu (in particular the following γ rays were used : 1332.5, 1791.6, 2158.9 and 3124.1 keV).

3) ANALYSIS OF DATA

3.1. Yield functions : They were measured at 23, 27, 32, 36 and 40 MeV. Fig. 2 shows the relative intensity of some γ rays. It may be noted that the 1660 keV γ depopulating a $J^\pi = 5^+$ state has a decreasing yield function reactions because the 1173 KeV ray intensity is mainly due to high-spin levels ($J^\pi \geq 7^-$).

3.2. Anguler distributions : They were performed at 8 angles from 30° to 150°, on an isotopic target with Bi backing in order to reduce Doppler shifts. Results of the analysis are gathered in Table 1. Formula and sign convention of Yamazaki [10] have been used.

3.3. γγ coincidences : An electronic timing measurement has shown no isomeric levels with $T_{1/2}$ > 2 ns. Thus, prompt γγ coincidences are sufficient to establish the level scheme. The data were recorded on magnetic tapes in the 2048 x 2048 format (E_γ up to 2 MeV with one Ge(Li) and up to 4 MeV with the other one). The two GeLi detectors were perpendicular to the beam axis. The angle between them was 90° and they were seperated by a thick sheet of Pb : in this way, the 511-511 keV coincidence from β^+ decay of ^{60}Cu and the back-scattering from one detector to the other were strongly reduced. Fig. 3 and Fig. 4 present some selected spectra observed in coincidence with events in the indicated regions backgrounds being substracted.

3.4. DSAM lifetime measurements : The method exposed at length in ref. 11 uses the fact that the target is self-supported to extract rather good stopping powers which usually are the chief weakness of DSAM. The 0.9 mg/cm^2 target thickness is comparable to the 0.45 mg/cm^2 range of nuclei recoiling with the center of mass velocity. The Doppler broadened peak shape is independent (χ^2 only changes less than 1 %) on the lifetime τ provided that τ is longer than a limit $\tau_1 \approx 10$ ps because the Doppler shifted peak is then solely due to the nuclei recoiling into the vacuum.

the unshifted peak counting the nuclei stopped inside the target. So the 1084 keV peak in ^{60}Ni measured by Moyat et al. [3] (423 ± 70) ps and by Kearns et al [4] (360 ± 30) ps may be fitted to extract the nuclear stopping power which is assumed to show the following pattern : $d\varepsilon/d\rho = ax/\exp(x^2/2)$ with $x = b\varepsilon^{1/2}$ (see fig. 5). Whatever unprecise the long lifetime is, rather safe stopping powers can be extracted and then used to get better DSAM measurements of unknown lifetimes. Results are listed in Table 2.

When the apparent lifetime τ_a is close to the limit τ_l (in the range $2 < \tau_a < 10$ ps) i.e. when the distorted peak is closely shaped to the above mentionned limit, the determination of τ becomes uncertain. The limitations on τ could be extracted from comparison between spectra obtained with self supporting target and Bi-backed target. Indeed, from a DSAM point of view, prompts γ rays ($\tau < 2$ ns) may have two asymptotical behaviours :

i) "long lifetimes" γ rays ($\tau_a > 4$ps) where Doppler shift is mainly due to emitting nuclei going out from the 0,9 mg/cm^2 target as mentionned above. (This value $\tau_a = 4$ ps is different from $\tau_l = 10$ ps, because it is the upper limit of the reliable measurement range through DSAM).

ii) "short lifetimes" γ rays ($\tau_a < 0.6$ ps) for which the Doppler effect is essentially due to nuclei recoiling inside the target (this limit is the stopping time of a ^{60}Ni nucleus recoiling in ^{58}Ni with the center of mass velocity). The dispersion of the recoiling nuclei velocities due to the evaporated particles does not change too much these upper and lower limits in the cases

of (pn) or (2p) evaporation.

The effect of adding a backing to the self supporting target is quite different on the Doppler peak shape for these two asymptotical categories : it suppresses the Doppler shifted peak of the i) category because of the strong stopping powers of Bi, so the unshifted peak remains alone in the spectra whatever the detector angle is. On the other hand the Bi-backing does not affect the peak shape of category ii).

Hence comparison between peak shapes obtained at forward and backward angles with self-supporting or Bi-backed targets brings the following lifetime informations.

- i) if the Bi-backing suppresses the Doppler shifted peak, the apparent lifetimes τ_a is longer than 4 ps (for $\tau_a > 4$ ps, no shape difference is perceptible).
- ii) if the Bi-backing does not change the relative height of the Doppler shifted peak, the apparent lifetime τ_a is shorter than 0.6 ps.
- iii) if the Bi-backing partly suppresses the Doppler shifted peak, the apparent lifetime τ_a is limited $0.6 < \tau_a < 4$ ps.

On fig. 6 the comparison between single spectra got with a self supporting target and prompt spectra obtained with a Bi backed target shows that

- the 1224 keV γ ray in ^{57}Co belongs to the ii) category (τ = 0.08 ps, τ_a = 0.6 ps)
- the 1084 keV γ ray in ^{60}Ni belongs to the i) category (τ = 400 ps).

4) SPIN-PARITY ASSIGNMENTS

Spin-parity assignments have been deduced with more or less reliance using :

- the fact that in the fusion evaporation reactions, γ cascades usually proceed from higher to lower spin
- the angular distribution measurements (see Table 1)
- the yield functions : increasing slope corresponds to increasing spin
- the lifetime measurements or estimations (see Table 2)
- the coherence of the established level scheme

The deduced level scheme is shown in Fig. 7. Table 3 presents the branching ratios of some levels in ^{60}Ni. Because the lower states are well known, we only discuss levels with excitation energy higher than 4 MeV.

- The 4165.2 keV level : The assignment $J^{\pi} = 5^{+}$ of Barker et al. [12] is confirmed because of the undoubtedly M1/E2 character of the 1660 keV γ ray ($A_2 = -1$, $\delta = 2.1$) in agreement with Kearns et al. [4]. Our limits set on the lifetimes through DSAM $1.2 < \tau < 4$ ps is in the vicinity of their measurement 1.2 ± 0.6 ps for which they neglected the effects of contamination.

- The 4264.9 keV level : Its belongs to the so called C Yrast cascade and the assignment $J^{\pi} = 6^{+}$ of Moyat et al. [3] and Kearns et al. [4] is obviously confirmed, and also a weak branch of 4 % which decays to the 4_2^{+} state at 3120 keV through a 1145 keV transition.

- The 4407.2 keV level : Three γ rays are issued from this weakly fed new state, none of them have reliable angular distributions. It may only be suggested from poor arguments (angular distribution, weak populating, levels which feed or are fed by this state) that the spin may be (5,6).

- The 4985.9 keV level : Recently reported by Kearns et al. [4] who suggested $J^{\pi} = 6^{+}, 8^{+}$, this state might be the 5050 keV ($J^{\pi} = 6^{+}$) level seen via ^{60}Ni (e,e') by Torizuka et al. [13]. The 80 % branch E2 transition (2480 keV, A2 = 0.2, τ = 1.5 ps) we found to decay to the $J^{\pi} = 4^{+}$ Yrast level, wholy confirms $J^{\pi} = 6^{+}$.

- The 5014.8 keV level : This new level, not seen in H.I. induced or direct reactions decays to three 4^{+} levels and perhaps to the 2^{+} level at 2159 keV. The 1895 keV γ ray has L = 1 character. The 2509 keV transition to the 4^{+} Yrast state is perturbed by another γ ray of about the same energy in ^{60}Cu but the 334 keV γ ray issued from the 7^{-} Yrast state which feeds the 5014 keV level has neat enough E2 character (A2 = 0.19) to make sure of the $J^{\pi} = 5^{-}$ assignment to this new level. The transition intensities deduced from its lifetime $\tau < 0.3$ ps are usual for E1 transitions (see Table 3) according to the recently compiled values in the 45-90 mass region by Endt [14]. The hypothetical E3 2856 keV γ ray has not been clearly seen in coincidence with the 334 keV gate, but this gate shows a line at 826 keV which is also present in prompt spectra with a much greater intensity than it should be for a pure ^{60}Cu radioactivity line (the 467 keV is missing).

- The 5148.5 keV level : This new level decays through two γ rays. The 2643 keV line has likely the L = 2 character (A_2 = 0.34 ± 0.11). The long lifetime (4 ps < τ < 2 ns) would exclude the E2 character and thus give $J^\pi = (6^-)$ to this level. This assignment may be trusted by the probable M1/E2 character of the 200 keV transition which feeds this level from the $J^\pi = 7^-$ Yrast level.

- The 5348.8 keV level : From this work, nothing can be added to the characteristics of this well known Yrast $J^\pi = 7^-$ state (polarization by Moyat et al. [3] and RDM lifetime by Moyat [3] and Kearns [4] have utterly ruled out the $J^\pi = 7^+$ characteristics suggested by Ivanov. et al. [2].) However we establish that this longlived state decays in 5 distinctive ways (two of them were known so far [4]). One branch is a 2843 keV E3 transition to the $J^\pi = 4^+$ Yrast state (see Table 3), we notice that its angular distribution has an E3 transition behaviour ($A_2 >> 0$ and $A_4 \gtrsim 0$) see Table 1). This $J^\pi = 7^-$ level might be identified to the most strongly excited state seen at (5.52 ± 0.10) MeV by Van Driel et al. [15] via (α,^{2}He) and at 5.4 MeV by Ost et al. [16] via the (^{13}C,^{11}C) reaction.

- The 5863.4 keV state : We confirm the existence of this level already seen by Kearns et al. [4]. The characteristics $J^\pi = (7^+)$ are quasi-certain with regard to the M1/E2 1397 keV transitions (A_2 = -0.6 δ = -0.3). We add another branching of 60 % : 676 keV to the 6^+ state at 4986 keV, unfortunately perturbed by a γ ray in ^{57}Co. The measured τ = 1 ps lifetime of this level gives transitions intensities which only excludes J = 8 but does not allow to choose between E1 and M1 (see Table 3).

- The 6460.3 keV state : The 798 keV γ ray is perturbed by a line belonging to the ^{59}Ni and no spin assignment can be deduced. However Kearns et al. [3] saw this line on the 721 keV gate (which is correct) and thus built a level 798 keV above the 4986 keV state (which is wrong because the 798 keV is also seen in coincidence with the 676 keV and 1398 keV lines). They found that the 798 keV γ-ray has M1 character, which would assign $J^{\pi} = (8^{+})$ to this new level.

- The 6810.7 keV state : Our results confirm thoroughly the characteristics $J^{\pi} = 9^{-}$ assigned by Moyat [3] and Kearns [4] to this level which was the last one of the C cascade they saw in H.I. reactions. Only one discrete weak line quaintly appears to feed this strongly populated state.

- The 6836.6 keV state : The L = 1 character of the 1488 keV γ transition issued from this new level can not be surely established from angular distribution analysis. The increasing of its yield function suggests J = (8) but the Weisskopf estimate ($|M|^2 = 10$) of the 1488 keV transition if it were E2, cannot exclude J = 9.

- The 8043.8 keV state : This new level decays via two weak γ rays. The angular distributions analysis seems to lead to conflicting results with both L = 2 (A2 > 0) transitions. The J = 9 suggestion may be supported by the increasing slope of the yield curve and would give a correct Weisskopf estimate of the 2695 keV γ ray intensity if it were E2 (and thus gives negative parity to the level).

- The 8520.6 keV state : No reliable information can be extracted from the 1710 keV γ ray leading to the $J^{\pi} = 9^-$ Yrast state. However the angular distribution of the 477 keV gives clearly L = 1, its lifetime excludes the E2 character, so that the spin of the 8520.6 keV state would be J = 10 if the 8043.8 keV state were J = 9.

- The 9132.2 keV state : The angular distribution of the 612 keV γ ray suggests a L = 1 (M1/E2 ?) transition , and lifetime conditions also exclude the E2 character. The rapidly increasing yield function therefore suggests J = (11).

- The 9989.5 keV state : This latest top level reached via the (α,2p) reaction beyond the proton emission threshold, ($E_p \sim 9.5$ MeV), decays through a 857 keV line without reliable angular distribution. Yet the E2 character may be ruled out with regard to the $|M|^2 = 420$ corresponding intensity unacceptable for such high spin levels in quasi spherical nuclei.

To conclude, the spin of the 8044, 8521, 9132, 9990 keV levels is either 10, 11, 12, 13 or 9, 10, 11, 12 (what we effect).

5) CONCLUSION

First the striking features of experimental results will be noticed out and then tentatively explained by means of shell-model considerations.

5.1. Experimental results

If heavy ions had led to the gross structure of the level scheme so far, i.e. mainly the C Yrast cascade, the (α,2p) reaction brought many refinements, witness the unusual high number of levels with branching ratios in an even-even nucleus. The most striking case is that of the 5348.8 keV $J^{\pi} = 7^-$ level which presents 5 branching transitions.

Among those branching γ rays is found a 2843 keV E3 transition. According to the recent compilation of Endt [14] through the 45-90 masses an E3 connecting high-spin states is unusual, indeed most of known E3 lead to the ground state and were seen via Coulomb excitation and radioactivity. The $|M|^2 = 0.3$ Weisskopf estimate of this E3 transition lies in the average of the values given by Endt [14]. Looking back at the level scheme it is striking that the Yrast levels at 5349 keV and 6811 keV both collect 42 % and 21 % of the total γ intensity which feeds the 4^+_1 state, while neighbouring levels are very poorly populated. This may be particularly noticed about the two cascades :

i) 4986 keV 6^+ - 5662 keV (7^+) - 6460 keV (8^+) - 7431 keV (9^+)

ii) 8044 keV (9)- 8521 keV (10) - 9132 keV (11) - 9990 keV (12)

This strong difference of the intensities feeding those cascades and the $J^{\pi} = 7^-$ and 9^- Yrast levels is insufficiently accounted for by the poor supply of high angular momentum from α induced reactions, but must have a structure explanation. One possible interpretation is that the lost of intensity corresponds to a change of seniority (seniority 2 for 7^-, seniority

4 for 9^- with ^{56}Ni inert core) or to the breaking of ^{56}Ni (the i) and ii) cascades might correspond to a seniority of 4 with the broken ^{56}Ni core. See discussions below).

5.2 Tentative theoretical interpretation

5.2.1. The $J^\pi < 5^+$ states

For positive parity states with $J^\pi < 4^+$ shell model calculations of Koops et al. [6] have given nice agreement with experiment for excitation energies as well as for electromagnetic properties although they restrict the configuration space of the four extra-core neutrons to the $2p_{3/2}$, $1f_{5/2}$ and $2p_{1/2}$ orbits surrounding the ^{56}Ni inert core. In this way they also account for the $J^\pi = 5^+$, 6^+ states. (see Table 4). The energy of the Yrast $J^\pi = 6^+$ state predicted at 3.92 MeV may be compared with that of 4.265 MeV experimentally observed but its E2 transition rate is well described by ASDI. The second 6^+ state which they reckon at 4.95 MeV by MSDI may be the state found at 4.986 MeV. For $J^\pi = 5^+$ states, the state at 4.165 MeV is a good candidate for the level predicted at 4.03 MeV by MSDI although the calculated electromagnetic M1 and E2 rates are too strong. The second $J^\pi = 5^+$ state reckoned at 4.39 MeV may be the 4.407 experimental level.

5.2.2. The $J^\pi = 5^-$, (6^-), 7^-, 9^- states

Just above 5 MeV excitation appear negative parity states 5^-, (6^-), 7^-, as predicted by Ram Raj et al. [7] with the modified Tam-Dancoff approximation using extra-core neutrons in the $p_{1/2}$, $f_{5/2}$ and $g_{9/2}$ orbitals. We notice also that their excitation energies are in quite good agreement with the very

recent shell-model calculations in the $p_{1/2}$, $p_{3/2}$, $f_{5/2}$, $g_{9/2}$ space of Potbhare et al. [9]. Many arguments confirm the interpretation of the Yrast 7^- and 9^- states as members of a rotational aligned negative-parity band formed by coupling a $g_{9/2}$ and an $f_{5/2}$ neutron to the core. In this mass region far from well deformed nuclei able to bring high spin collective states, the cheapest way to build negative parity states in the shell model framework, is to call for the positive $g_{9/2}$ subshell at 3.7 MeV excitation in ^{57}Ni. Recently via the two neutron transfer reaction ^{58}Ni(α,^{2}He)^{60}Ni, Van Driel et al. [15] clearly established the two-neutron configuration of a state at 5.52 MeV. Indeed such a direct reaction at E_α = 65 MeV is known to strongly select states for which both nucleons couple their spin at maximum. Van Driel et al. [15] performed DWBA calculations and found that the 5.52, 8.92, 9.80 and 10.85 MeV states angular distributions agree with a L = 8 transfer. However they would also be compatible with a $J^\pi = 7^-$ state. The energy discrepancy with the 7^- Yrast level at 5.35 MeV can be accounted for by a poor resolution and an important background which makes calibration and identification difficult : Van Driel et al. [15] saw the $J^\pi = 4^+$ Yrast level at 2.51 MeV instead of 2.50 MeV, hence the highly excited state at 5.52 MeV is undoubtedly the $J^\pi = 7^-$ Yrast one if the error is extrapolated at higher energies.
The same two-neutron high-spin state has also been strongly selected at 5.4 MeV by Ost et al. [16] via the (^{13}C,^{11}C) reaction at $E_{^{13}C}$ = 105 MeV. In order to confirm that the above $J^\pi = 5^-$ and 7^- states have $[p_{1/2}, g_{9/2}]_{5^-}$ and $[f_{5/2}, g_{9/2}]_{7^-}$ configurations it is interesting to follow the energy evolution of these states

through the Ni, Zn, Ge isotopes on Fig. 8a. With increasing number of neutrons, their excitations energies curves have a weaker slope than the $g_{9/2}$ single particle energy in the corresponding element, which is well explained by a slightly increasing pairing energy (Fig. 8b). In the absence of shell-model calculations including the $g_{9/2}$ orbit, we have proposed a crude shell-model in order to account for two-nucleon high-spin states through the Z = 28 - 32 range.

The excitation energy of a two-nucleon state with maximum spin coupling, is simply calculated as the sum of the experimental energies of each nucleon in its single-particle state in the neighbouring nucleus plus the pairing energy : for example $E[\nu f_{5/2}, \nu g_{9/2}]^{7^-} = E(\nu f_{5/2})_{5/2^-} + E(\nu g_{9/2})_{9/2^+}$ + Pairing. The agreement between experimental and reckoned values of excitation energies is illustrated on Fig. 8c. The worse case is that of the ^{60}Ni nucleus where the theoretical-experimental difference only reaches 10 % for the $J^\pi = 5^-$ level).

In order to argue about the sudden appearing of the $g_{9/2}$ neutrons in these 5^-, (6^-), 7^- states near 5 MeV, we may at last consider the hindrance of the transition rates to lower levels. Among the five branching of the 7^- state, the E2 value of 6 Wu to the 5^- level and the probable M1 value of 3.4 10^{-4} Wu to the (6^-) level are right in the averages over the A = 25 - 90 nuclei according to Endt [14]. But the hindrances of the E1 transitions to levels which are not assumed to involve the $g_{9/2}$ orbital are found very strong : 3.10^{-6} and 10^{-6} Wu. From the 0.3 Wu of the E3 transition down to $J^\pi = 4^+$ Yrast level, no conclusions

can seriously be derived with regard to the poor statistic of E3 transitions, most of them being $3^- \rightarrow 0^+$ transitions. For $9/2^+ \rightarrow 3/2^-$ transitions safe results in ^{75}As, ^{77}As, ^{77}Br, ^{71}Br give respectively 0.063 - 0.22 - 0.016 - 0.03, which are close to our 0.3 Wu.

The last strongly populated level, i.e. the 9^- Yrast top state of the C cascade, is likely to have a configuration which involved $g_{9/2}$ neutrons with probably the $[g_{9/2}, f_{5/2}, (f_{5/2}, p_{3/2}, p_{1/2})^{2^+}]_{9^-}$ configuration since it appears to be strongly connected with the 7^- Yrast state which is $[g_{9/2}, f_{5/2} (f_{5/2}, p_{3/2}, p_{1/2})^{2^+}_{0^+}]_{7^-}$ by an E2 transition of 10 Wu.

5.2.3. The tentative $f_{7/2}^{-1}$ neutron holes cascades

It has already been noticed that the so called i) and ii) cascades (see 5.1) are very poorly fed with respect to the 7^-, 9^- above levels. Yet in the i) cascade the 6480 keV state is likely to be a $J^\pi = 8^+$ Yrast state and should be more populated. It is tempting to explain this difference of feeding by a difference of structure which would exchange the effect of high energy and high-spin states.

Indeed there would be no wonder if the above shell-model with 4 neutrons in the $p_{1/2}$, $p_{3/2}$, $f_{5/2}$, $g_{9/2}$ orbitals surrounding a ^{56}Ni core were extended with core excitations, since the 2.7 MeV energy of the first $J^\pi = 2^+$ excited state in ^{56}Ni is lower than the 3.7 MeV single particle $g_{9/2}$ orbitel in ^{59}Ni. Such 2.7 MeV energy jumps happen in ^{60}Ni level scheme at the bottom of the i) and ii) cascades with 2.48 MeV

and 2.695 MeV respectively.

For the i) cascade the $6^+ \rightarrow 4^+$ E2 transition has an intensity of 0.3 W.u. which may be compared to the 6 W.u. of the $2^+ \rightarrow 0^+$ E2 γ-ray in ^{56}Ni (the E2 rate is hindered by the competing M1 721 keV transition). The main configuration of the 2^+ state in ^{56}Ni probably is $(p_{3/2}, f_{7/2}^{-1})_{2^+}$ and using the likely $(f_{5/2})^2_{2^+}$ configuration of the 4^+ Yrast state in ^{60}Ni the above picture allows to build the states

$$[(f_{5/2})^2_{4^+} \times (p_{3/2}, f_{7/2}^{-1})_{2^+,3^+,4^+,5^+}]_{6^+,7^+,8^+,9^+}$$

at 4.98, 5.66, 6.46 and 7.43 MeV respectively.

In ^{58}Ni where only 2 neutrons are outside the ^{56}Ni core, a similar situation may happen. Indeed a 2668 keV γ ray connecting $J^\pi = 6^+$ and 4^+Yrast states, was suggested by Kim et al. [18] (but not confirmed later [19]). The 6^+ state then might be also interpreted as $[(f_{5/2})^2_{4^+} \times (f_{7/2}^{-1}, p_{3/2})_{2^+}]_{6^+}$.

In ^{60}Ni such a picture would nicely agree with rates of pure M1 trahsitions connecting the levels of the i) cascade when angular distribution analysis and transitions rates (Tables 2 and 3) are considered.

A similar attempt may be done to interpret the ii) cascade states with also configurations containing holes in the $f_{7/2}$ orbital. These configurations would be :

$$[(g_{9/2}, f_{5/2})_{7^-} \times (p_{3/2}, f_{7/2}^{-1})_{2^+,3^+,4^+,5^+}]_{9^-,10^-,11^-,12^-}$$

For comparison with $J = 2^+$ level at 2.7 MeV in ^{56}Ni, the 8044 keV level lifetime in ^{60}Ni is rather badly determined, but the above transitions connecting the levels of the ii) cascade could fairly be M1.

One of the experimental evidences for the above interpretation of the i) and ii) cascades is the results of Chang et al. [20] obtained via (α,t) and (α,He^3) on ^{58}Co at $E_\alpha = 120$ MeV. These reactions are known to favour excitation of states with a particle in the high l orbitals and Chang et al. [17] thought that they populated $(f_{7/2}^{-1}, g_{9/2})$ levels in the $E_x = 5 - 7$ MeV range in ^{60}Ni. Now, using electron scattering measurements, Lindren et al. [18] found $(g_{9/2}, f_{7/2}^{-1})_{8^-}$ states at 7.55, 8.45, 12.36, etc.. MeV energies. This first 8^- state at 7.55 MeV lies 1 MeV above the likely $J = 8$ states at 6.46 and 6.83 MeV and cannot be populated through $(\alpha,2p\gamma)$ because the fusion-evaporation process only reaches Yrast or quasi-Yrast levels. Nevertheless the two above mentionned experiments establish that $f_{7/2}^{-1}$ neutron hole exists in the 5-10 MeV excitation range and would certainly interfere in the configurations of the i) and ii) cascades in a way very close to that we indicate.

REFERENCES

[1] Auble, R.L., Nucl. Data Sheets 28, 103 (1979)

[2] Ivanov M.A., Lemberg, I.Kh.,Meshin, A.S., Peker, I.K., Chuganov, I.N., Izv. Akad. Nauk. SSSR [ser fiz.] 39, 1965 (1975)

[3] Moyat G.,Delaunay B., Delaunay J., Eberth, J., Zobel, V., Cleeman, L., Nucl. Phys. A318. 236 (1979)

[4] Kearns, F., Ekstrom, L.P., Gones, G.D., Morisson, T.P., Mustaffa, O.M., Price, H.G., Simister, O.N., Twin, P.J., Wadsworth R., Ward, N.J., J. Phys. G., 6, 113 (1980)

[5] Hansen, D.L., Nelson Stein, Sunier, J.W., Woods, G.W., Ole Hansen, Nucl. Phys. A321, 472 (1979)

[6] Hansen, D.L., Nelson Stein, Woods, G.W.,Sunier, J.W., Ole Hansen, Nilson, B.S., Nucl. Phys. A336, 290 (1980)

[7] Ram Raj, Roy, B.B., Rustgi, O.P., Rustgi, M.L. Lett. Nuovo Cim 23, 12 (1978)

[8] Koops, J.E. and Glaudemans, P.W., Z. Phys. A280, 181 (1977) Koops, J.E. Thesis Utrecht (1978)

[9] Potbhare, V., Sharma, S.K., Pandya, S.P., Phys. Rev. C24, 2355 (1980)

[10] Yamazaki, T., Nucl. Data A3, 1 (1967)

[11] Morand, C. and Tsan Ung Chan., Comp. Phys. Com. 23, 393 (1981)

[12] Barker, J.H. and Sarantities D.G., Phys. Rev. C9, 607 (1974)

[13] Torizuka, Y., Kojima, Y., Oyamada, M., Nakahara, K., Sujiyama, K., Terasawa, T., Itok, K., Yamaguski, A. and Kimura, M., Phys. Rev. 185, 1499 (1969)

[14] Endt, P.M., Atom. Nucl. Data Tables 23, 547 (1979)

[15] Van Driel, J., Kamermans, R., de Meijer, R.J. and Morsh, H.P., Nucl. Phys. A350, 109 (1980)
Annual Report 1977 and 1979 Groningen (unpublished)

[16] Ost, R.A., Sanderson, N.E., England, J.M.A., Nelson, J.M., Fulton, B., and Morrison, G.C.
Annual Report, Birmingham (1975) unpublished

[17] Tsan Ung Chan, Agard, M., Bruandet, J.F., and Morand, C., Phys. Rev. C, 19, 244 (1979)

[18] Kim, A.J.
Oak Ridge Annual Report (1975) unpublished

[19] Ballini, R., Bendjaballah, N.,Delaunay, J., Fouan, J.P., and Tokarevski, W., Nucl. Phys. A258, 388 (1976)

[20] Chang, C.C., Collons, M.T., Koontz, R.W., Wu, J.R. Holngren, H.D., Bull. Am. Phys. Soc. 24, 631 (1979)

[21] Lindgren, R.A., Plum, M.A., Hicks, R.S., Parker, B., Peterson, G.A., Moruyama, X.K., Williamson, C.F., Proc. of the Int. Conf. on Nucl. Physics, Berkeley, California (1980) p. 79

Table 1

RESULTS OF THE ANGULAR DISTRIBUTION MEASUREMENTS

E_γ	E_i	E_f	I_γ	$A_2 \pm \Delta A_2$	$A_4 \pm \Delta A_4$	$J_i \to J_f$	$\delta \pm \Delta\delta$	Multipolarity and rem
200.3	5348.8	5148.5	1.4	- 0.44 ± 0.09	- 0.3 ± 0.16	$7^- \to 6^+$	$-0.17\ ^{-0.5}_{+0.2}$	
242.0	4407.2	4165.2	1.5	- 0.06 ± 0.3	0.53 ± 0.35	5		
334.0	5348.8	5014.8	8.1	0.19 ± 0.07	-0.12 ± 0.11	$7^- \to 5^-$	$-0.1\ ^{-0.15}_{+0.1}$	E2
362.9	5348.8	4985.9	3.1	- 0.32 ± 0.06	-0.02 ± 0.09	$7^- \to 6^+$	$-0.07\ ^{-0.5}_{+0.3}$	E1
467.2	2626.0	2158.8				$3^+ \to 2^+$		Rad ^{60}Cu
476.8	8520.8	8043.8	5.3	- 0.32 ± 0.04	-0.10 ± 0.06	(10) → (9)	$-0.03\ ^{+0.10}_{+0.10}$	
498.0	3124.0	2626.0				$2^+ \to 3^+$		Rad ^{60}Cu
611.6	9132.2	8520.8	4.4	- 0.45 ± 0.08	-0.15 ± 0.13	(11) → (10)	$-0.1\ ^{+0.15}_{+0.15}$	
676.4	5662.3	4985.9				(7⁺) → 6⁺		perturbed by γ in ^{5}
721.0	4985.8	4264.8	∿2.2			$6^+ \to 6^+$		
737.0	4407.2	3670.2	∿3.5			→ (4)		
741.3	5148.5	4407.2	∿4			(6⁻) →		
798.0	6460.3	5662.3	8.1			8⁺ → 7⁺		perturbed by γ in ^{5}
857.3	9989.5	9132.2	4			→ (11)		
970.6	7430.9	6460.3				→ (8⁺)		
1383.9	5348.8	4264.8	30.5	- 0.40 ± 0.02	0.06 ± 0.03	$7^- \to 6^+$	$-0.1\ ^{+0.3}_{+0.1}$	E1
1145.2	4264.8	3119.7				$6^+ \to 4^+$		
1164.5	3670.2	2505.7				(4) → 4⁺		Perturbed by γ in ^{6}

3.2	2505.7	1332.5	100	-0.18 ± 0.05	- 0.09 ± 0.09	$4^+ \rightarrow 2^+$	-0.09 $^{-0.3}_{+0.5}$	E2
7.2	8043.8	6836.6	2	0.36 ± 0.17	0.17 ± 0.27			
3.5	2626.0	1332.5				$3^+ \rightarrow 2^+$		Rad ^{60}Cu
5	1332.5	0				$2^+ \rightarrow 0^+$		Important contribution from Rad ^{60}Cu
1.6	5014.8	3670.2	0.5			$5^- \rightarrow 4^+$		
7.4	5662.3	4264.9	3.3	- 0.63 ± 0.14	0.28 ± 0.17	$(7^+) \rightarrow 6^+$	-0.3 $^{-0.5}_{+0.2}$	M1/E2
1.9	6810.7	5348.8	21.4	0.22 ± 0.04	0.03 ± 0.21	$8^- \rightarrow 7^-$	-0.1 $^{-0.15}_{+0.2}$	E2
7.8	6836.8	5348.8	4.7	- 0.11 ± 0.12	0.2 ± 0.18			
1.5	4165.2	2505.7	5.3	- 1.0 ± 0.1	0.43 ± 0.09	$5^+ \rightarrow 4^+$	-1 $^{-0.4}_{+0.5}$	M1/E2
9.9	8520.6	6810.7	1.5			$\rightarrow 9^-$		
1.2	4264.9	2505.7	45.0	0.21 ± 0.04	- 0.11 ± 0.07	$6^+ \rightarrow 4^+$	-0.1 $^{-0.2}_{+0.4}$	E2
7.2	3119.7	1332.5	11	0.13 ± 0.07	- 0.05 ± 0.12	$4^+ \rightarrow 2^+$	-0.18 $^{+0.2}_{+0.5}$	E2
1.5	3124.0	1332.5				$2^+ \rightarrow 2^+$		Rad ^{60}Cu
5.1	5014.8	3119.7	2.4	- 0.53 ± 0.07	0.14 ± 0.09	$5^- \rightarrow 4^+$	-0.18 $^{-0.2}_{+0.2}$	E1
1.5	4407.2	2505.7	1	- 0.04 ± 0.3	0.2 ± 0.3	$\rightarrow 4^+$		
5.8	2158.8	0				$2^+ \rightarrow 0^+$		Rad ^{60}Cu
1.2	4985.9	2505.7	8.7	0.30 ± 0.08	- 0.08 ± 0.1	$6^+ \rightarrow 4^+$		E2
5.2	5014.8	2505.7				$5 \rightarrow 4^+$		perturbed by γ in ^{60}Cu
3.8	5148.5	2505.7	2.8	0.34 ± 0.11	- 0.11 ± 0.18	$(8^-) \rightarrow 4^+$	0 $^{+0.25}_{+0.5}$	

15.0	8043.8	5348.8	2	0.4 ± 0.3	-0.3 ± 0.4			
43.1	5348.8	2505.7	0.8	0.40 ± 0.07	0.05 ± 0.10	$7^- \rightarrow 4^+$	$0\ ^{-0.25}_{+0.5}$	E3
24.0	3124.0	0				$2^+ \rightarrow 0^+$		Rad ^{60}Cu

E_γ transition decays from E_i state ($J^\pi = J_i$) to E_f state ($J^\pi = J_f$). A_2 and A_4 are coefficients of Legendre polynomials from $I(\theta) = I_o (1 + A_2 P_2 (\cos\theta) + A_4 P_4 (\cos\theta))$ with I_o (1173.2) = 100 intensity. The intensity of the 1173.2 keV γ lines is chosen for the normalization because the 1332.5 keV γ-line has an important contribution from the radioactivity of ^{60}Cu. Blank values for A_2 and A_4 mean that no reliable information can be deduced from angular distribution analysis.

LIFETIMES MEASUREMENTS OF ^{60}Ni LEVELS

	J^π	Eγ	$\theta_m°$	τ_m	τ_f	$\|M\|^2$ in W.U. : E1	M1	E2	Feeding ways A	B	τ_1	C	τ_2	D	τ_3	E	τ_4	Remarks
20	4^+	1787			<4*			>0.8										
65	5^+	1660	25	1.4<	1.2<2 <4*		$1.7\ 10^{-3}$	1.1	0.75	0.25	6							
			160	1<														
85	6^+	1759	25	0.5<2 <∞	0.6<3 <4 *			1.1	0.23	0.69	400	0.08	2					
			160	1<6 <∞														
97		737	25	2<4 <∞	4* < <2000+	<2.4 10^{-4}	<1.2 10^{-2}	< 40	0.9	0.1	400							mixed with the 741 keV ray
			160	<2 <10														
86	8^+	721	25	0.4<1 <15	0.5<1.5<5		$5.8\ 10^{-2}$		0.4	0.3	400	0		0.1	1	0.2	1.7	
			160	<1.7<10														
		2480	25	0.4<0.9< 3				0.3										
			160	0.8<1.8<10														
15	5^-	1895	160	0.06<0.25<1.5	0.1<0.3<4	$1.8\ 10^{-4}$			0.4	0.6	400							
		2509	25	0.14<0.5 <6		$4.7\ 10^{-5}$												
			160	0.1<0.3 <5														
45	(6^-)	2643	25	0.5<2	1* < <2000+			<4.5 10^{-2}	0.6	0.4	400							
			160	1<														
62	(7^+)	676	25	0.8<1.7<7	0.6<1 <4*	$1.2\ 10^{-3}$	$6.2\ 10^{-2}$	250	0.3	0.7	1.7							
			160	0.7<1 <3														
		1397	25	0.14<0.7<8		$8\ 10^{-5}$	4.10^{-3}	4										doubtful mixing ra
			160	0.2<1 <8														
80	(8^+)	798	25	1<1.85<4	1<1.7<4	$7.4\ 10^{-4}$	$3.7\ 10^{-2}$	110	1									
			160	1.1<1.8<4														
11	9^-	1462	25	0.68<0.88<1.3	0.6<0.9<1.5			10	0.76	0.07	0.8							mixed wi 1469 keV
			160	0.66<0.97<2														mixed wit 1454 keV

(8)	1488	25 160	0.5<0.67<0.8 0.6<1 <2	0.5<0.8<1.5	$2.4\ 10^{-4}$	$1.2\ 10^{-2}$	10	0.6	0.4	0.4					
(9)	1207 2695	25 25 160	0.05<0.5<2 <0.02<0.4 <0.02<0.3	<0.05<0.5	$3.6\ 10^{-5}$ $3.2\ 10^{-4}$	0.18 $1.6\ 10^{-2}$	230 4	0.2	0		0	0.25	0.7	0.55	0.3	Very weak a forward anc backward angles
(10)	477	25 160	0.5<0.8<1.5 0.25<0.5<1.5	0.4<0.7<1.5	$6.7\ 10^{-3}$	0.33	2700	0.4	0		0	0.2	0.26	0.4	0.3	
(11)	612	25 160	0.24<0.33<0.4 0.1<0.2<0.4	0.15<0.28<0.4*	$1.1\ 10^{-2}$	0.53	2600	0.3	0.7	0.3						mixed with 617 keV of ^{60}Cu
(12)	857	25 160	0.15<0.26<0.4 0.24<0.4< 0.8	0.2<0.3<0.8*	$3.4\ 10^{-3}$	0.17	420	1								

The measured lifetime level has E_x (keV) excitation energy and characteristics J^π. The Doppler distorted γ ray of E_γ (keV) issued from this level, gives at $\theta_m°$ degrees the measured lifetime value τ_m. τ_f is the adopted final value averaging the various τ_m according to confidence considerations such as lower X^2 fit and neatness of the peak. (In the inequalities τ_m and τ_f are the central value flanked by the lower and upper limits of the measurements. $|M|^2$ is the deduced Weiskopf intensitis of the transition E_γ. The following columns concern the feeding ways (intensities and lifetimes - see explanations in Ref. 11) τ are given in ps. The remarks implie wether the E_γ γ ray have been fitted at the same time as a neighbouring one. (see fig. 5). The asteriks denote the cases where one of the limits was extracted from the comparison between Doppler behaviours in spectra performed with either self supporting or Bi l :ked targets (see fig. 6). The crosses indicate the electronic limit τ < 2 ns.

Table 3

BRANCHING RATIOS AND WEISSKOPF INTENSITIES IN ^{60}Ni

E_i	J^π_i	τ_i(ps)	E_f	J^π_f	E_γ	BR	$\lvert M\rvert^2$ W.U. E1	M1	E2	E3	Remark
265	6^+	3	3120	4^+	1145	4			0.2		
			2506	4^+	1759	96			1.1		
407	(5/6)	4<	4165	5^+	242	20	$2.2\ 10^{-3}/0.11$				upper limits of $\lvert M\rvert^2$
			3670	(4)	738	60	$2.4\ 10^{-4}/1.2\ 10^{-2}/40$				
			2506	4^+	1902	20	$4.6\ 10^{-6}/2.3\ 10^{-4}/0.12$				
986	6^+	1.5	4265	6^+	721	20		$5.8\ 10^{-2}$			
			2506	4^+	2480	80			0.3		
015	5^-	0.3	3670	(4^+)	1345	10	$8.7\ 10^{-5}/4.4\ 10^{-3}$				gate 334 keV
			3120	4^+	1895	54	$1.6\ 10^{-4}$				
			2506	4^+	2509[a]	35	$4.7\ 10^{-5}$				
			2159	2^+	2854	1				2.10^2	
148	(6^-)	4<	4407	(5/6)	741	60					enor. 30 % on BR
			2506	4^+	2643	40		$<4.5\ 10^{-2}$			
349	7^-	360	5148	(6^-)	200	3		$3.4\ 10^{-4}$			
			5015	5^-	334	17			6		
			4986	6^+	363	8	$3\ 10^{-6}$				
			4265	6^+	1084	70	$1\ 10^{-6}$				
			2506	4^+	2843	2				0.3	
862	(7^+)	1	4986	6^+	876[b]	60	$1.2\ 10^{-3}/6.2\ 10^{-2}/250$				gate 798 keV
			4265	6^+	1397	40	$8\ 10^{-5}$ /4 10^{-3}/ 4				
044	(9)	<0.5	6837	(8)	1207	50	$3.6\ 10^{-4}/1.8\ 10^{-2}/23$				enor 30% on BR, lowe
			5349	7^-	2695	50	$3.2\ 10^{-5}/1.6\ 10^{-3}/0.4$				limits of $\lvert M\rvert^2$
521	(10)	0.7	8044	(9)	477	80	$6.7\ 10^{-3}/0.33/2700$				
			6811	9	1710	20	$3.6\ 10^{-5}/1.\ 10^{-3}/1.1$				

a) perturbed by a line in ^{60}Cu b) perturbed by a line in ^{57}Co

The remarks indicate where intensities could not been straightly extract from angular distribution analysis, but were estimated from concidence spectra. Otherwise errors on the B.R. are of 10 %.

Table 4

COMPARISON BETWEEN SHELL MODEL CALCULATIONS[a] AND EXPERIMENTAL RESULTS FOR 5^+ AND 6^+ STATES

	Excitation energies (MeV)			Decay properties $\|M\|^2$ W.u.						
						M1		E2		
J_i	exp	MSDI	ASDI	$\to J_f^\pi$	exp.	MSDI	ASDI	exp	MSDI	ASDI
5^+	4.165	4.03	3.36	4_1^+	$1.7\ 10^{-3}$	$4.6\ 10^{-3}$	$2.2\ 10^{-3}$	1.1	8.3	6.1
				3^+	b)			b)	5.8	5.2
	(4.407)	4.39	4.39							
6^+	4.265	3.92	3.93	4_1^+	0			1.1	3.4	1.2
	4.986	4.95	4.56							

a) Koops et al.[8]

b) not seen experimentally.

FIGURE CAPTION

Fig. 1
Single spectrum of the ^{58}Ni + α reaction at E_α = 32 MeV

Fig. 2
Relative yield functions of some γ rays in ^{60}Ni

Fig. 3
Selected spectra in coincidence with events in the indicated regions and with substracted background. (BS indicate back-scattering effects and (o) denote ^{60}Cu γ due to neighbouring gate at 617 and 1469 keV).

Fig. 4
Spectra in coincidence with gates corresponding to different branches of the 7^- state at 5348.8 keV

Fig. 5
The top row displays the extraction of nuclear stopping power parameters for DSAM. At forward (θ = 25°) and backward (θ = 160°) angles, the 1084 keV line has been fitted for different nuclear stopping powers parameters (b = EXPO = 0.8, 1., 1.1, 1.2 ; a = CAN in the 0.5 -2. range). Fig. 5a) gives the corresponding two χ^2 valleys in the CAN versus EXPO plane, with the χ^2 minimum numerical values. The selected nuclear stopping-power indicated by a circle arrowed as the optimum has EXPO = 1.1 and CAN = 1.08 ± 0.05). the incertitude has been deduced from the gap between the two curves. At each angle the lowest χ^2 minimum fits (figure in b). Lower fits illustrate lifetimes mesurements using the above extracted stopping power as well for well shaped line (1759 keV) as for bad shaped line (477 keV) due to . statistics. Two of them have been fitted mixed with a neighbouring line of known lifetime : the energy, the relative intensity and the lifetime of the perturbing line are written vertically at the full energy channel.

Fig. 6

The top spectra obtained with a Bi backed target are prompt spectra (i.e. recorded at the same time as the beam burts income on the target, which explains the absence of radioactivity). The botton singles spectra have been obtained with a self supporting target of ^{58}Ni. Comparison between them provides lifetime information.

Fig. 7

Decay scheme of ^{60}Ni as a result of the present measurements.

Fig. 8

The evolution of the $J^{\pi} = 5^-$ and 7^- states energies through the Ni, Zn and Ge isotopes when they are interpreted with $[(p_{3/2}, f_{5/2})_{0^+} \times (p_{1/2}, g_{9/2})^2_{5^-}]$ and $[(p_{3/2}, p_{1/2})_{0^+} \times (f_{5/2}, g_{9/2})^2_{7^-}]_{7^-}$ configurations. Fig. 8a displays this rather smooth evolution of the excitation energy, with a slightly smoother slope than the single particle neutron $g_{9/2}$ energy. This difference of slopes may be accounted for by the slightly increasing pairing energy and the weaker decreasing slope of the single particle neutron $f_{5/2}$ energy (fig. 8b). Nevertheless our crude shell model[14] agrees very well with experiment results except for the ^{60}Ni case where the discrepancy reaches 10 % for the $J^{\pi} = 5^-$ level. (Fig. 8c). In this model the energy of a two-nucleon configurations state is calculated as the addition of the single particle state energies taken from the neighbouring nuclei plus the pairing energy (if it is the case).

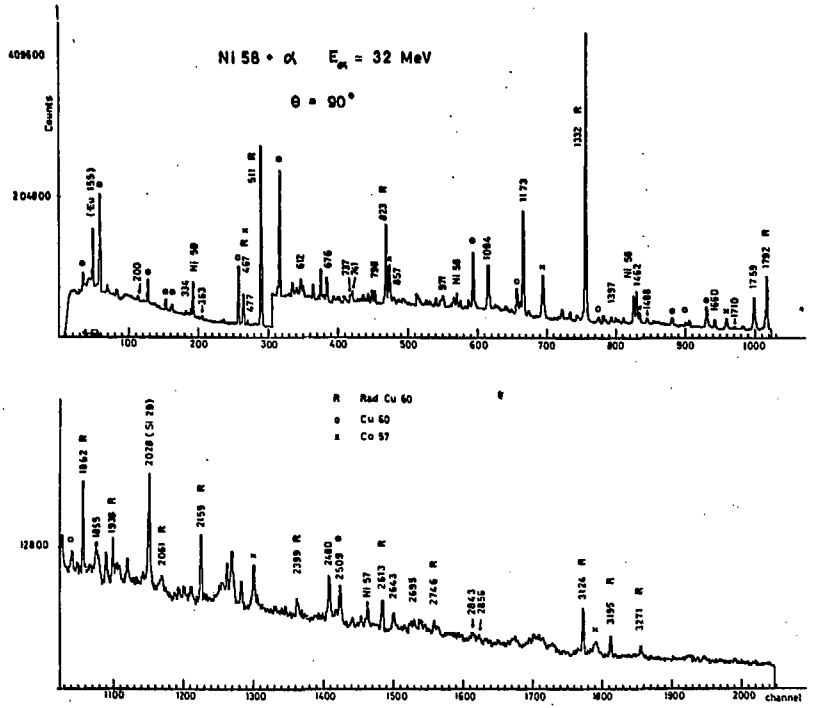
Ni 58 + α E_α = 32 MeV
θ = 90°
Counts
409600
204800
12800
(Cu 155)
200
334
353
Ni 58
477
487 R
511 R
612
676
727
741
798
823 R
852
971
Ni 58
1044
1173
1332 R
1397
Ni 58
1482
1488
1660
1710
1753
1792 R
R Rad Cu 60
o Cu 60
x Co 57
1862 R
1955
1938 R
2028 (Si 28)
2061 R
2159 R
2389 R
2640
2508
Ni 57
2613 R
2643
2695
2746 R
2843
2856
3124 R
3195 R
3271 R
channel

Fig 1

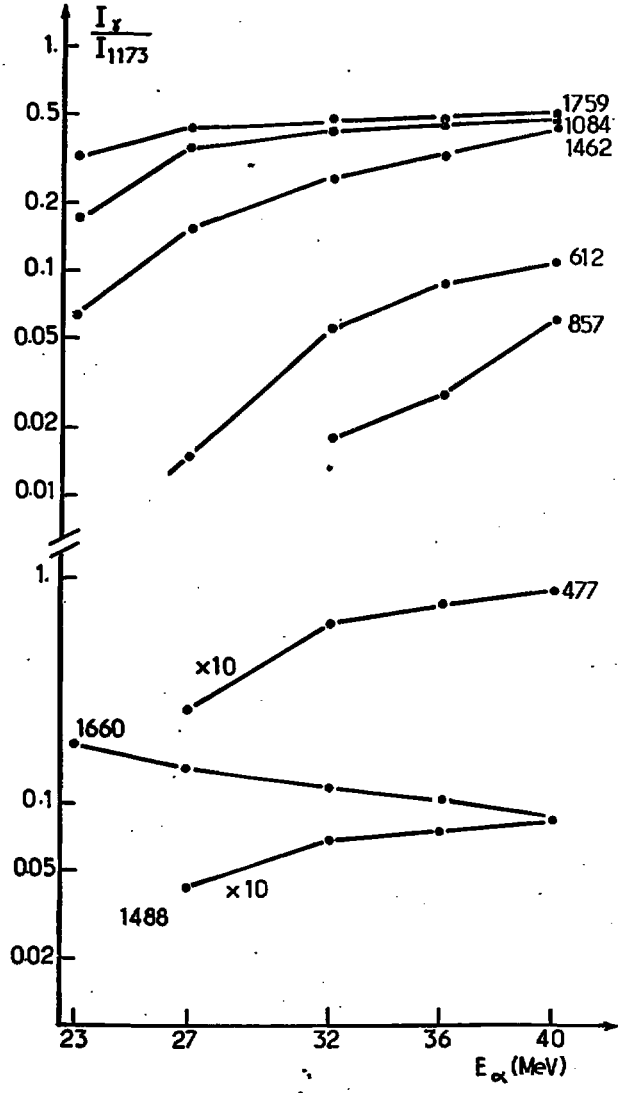
$\frac{I_\gamma}{I_{1173}}$
1.
0.5
0.2
0.1
0.05
0.02
0.01
1759
1084
1462
612
857
1.
477
×10
1660
0.1
0.05
×10
1488
0.02
23
27
32
36
40
E_α (MeV)

Fig 2

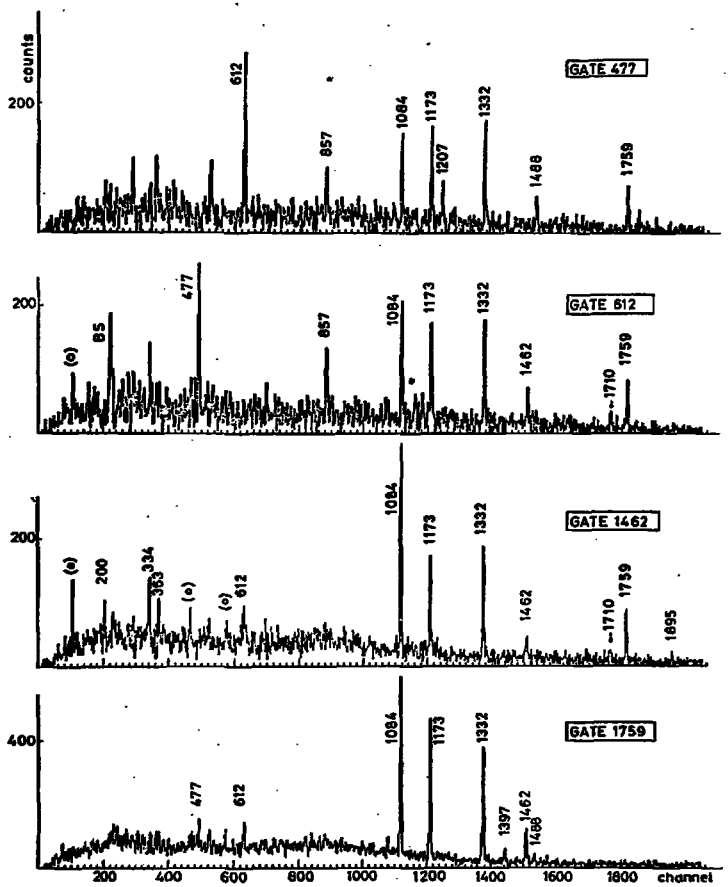
counts
200
612
857
1084
1173
1207
1332
1488
1759
GATE 477
200
(e)
85
477
857
1084
1173
1332
1462
1710
1759
GATE 612
200
(e)
200
334
383
(e)
(e)
612
1084
1173
1332
1462
1710
1759
1895
GATE 1462
400
477
612
1084
1173
1332
1397
1462
1488
GATE 1759
200
400
600
800
1000
1200
1400
1600
1800
channel

Fig 3

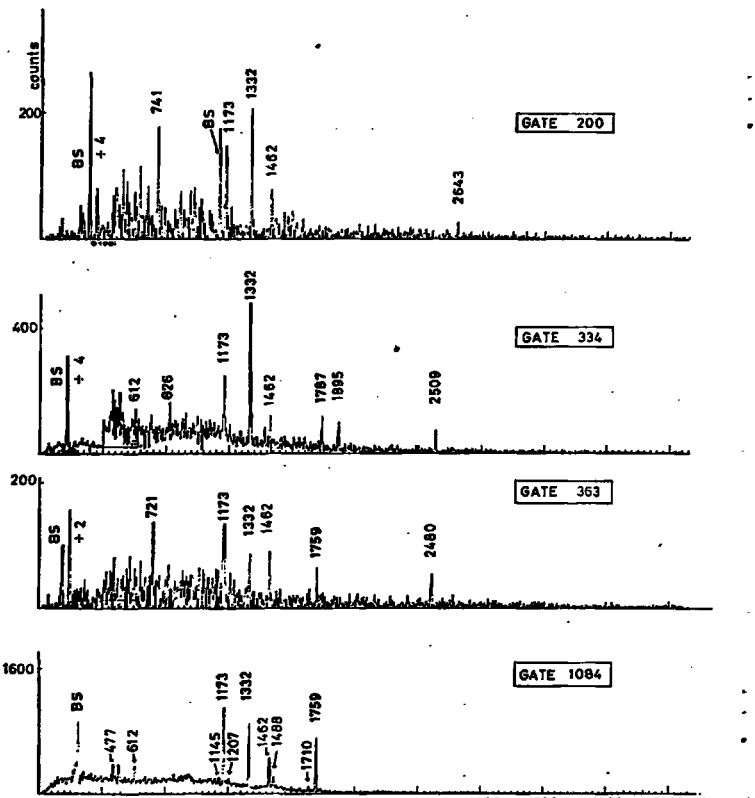
counts
200
BS
+ 4
741
BS
1173
1332
1462
2643
GATE 200
400
BS
+ 4
612
626
1173
1332
1462
1787
1895
2509
GATE 334
200
BS
+ 2
721
1173
1332
1462
1759
2480
GATE 363
1600
BS
477
612
1145
1173
1207
1332
1462
1488
1710
1759
GATE 1084
200
400
600
800
1000
1200
1400
1600
1800
2000
channel

Fig 4

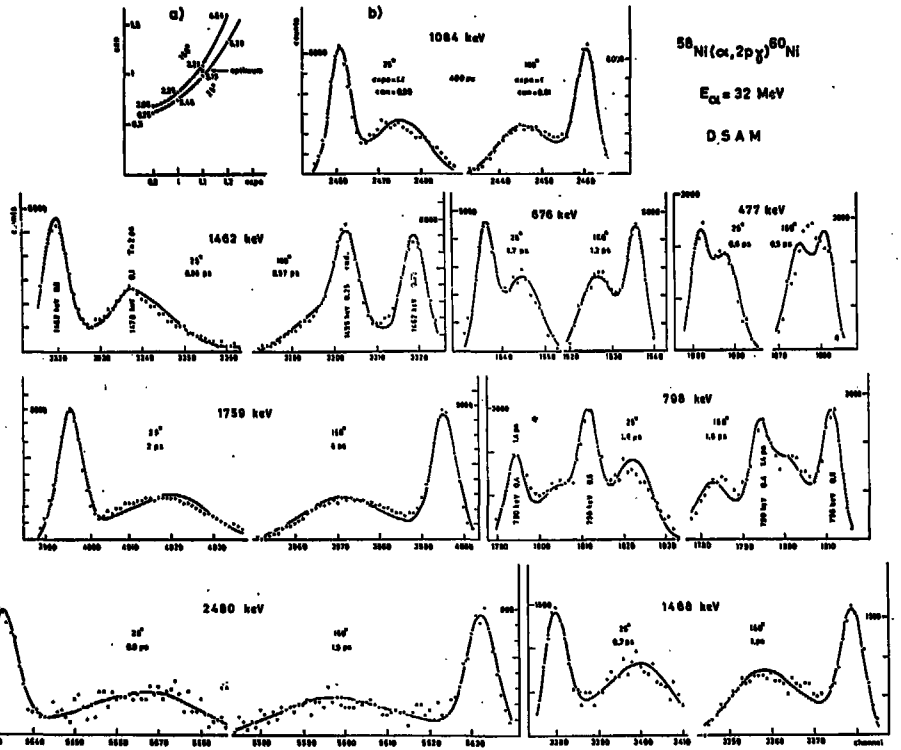
a)
b)
1084 keV
^{58}Ni(α,2pγ)^{60}Ni
E_{α} = 32 MeV
D.S.A.M
1462 keV
676 keV
477 keV
1759 keV
798 keV
2480 keV
1468 keV

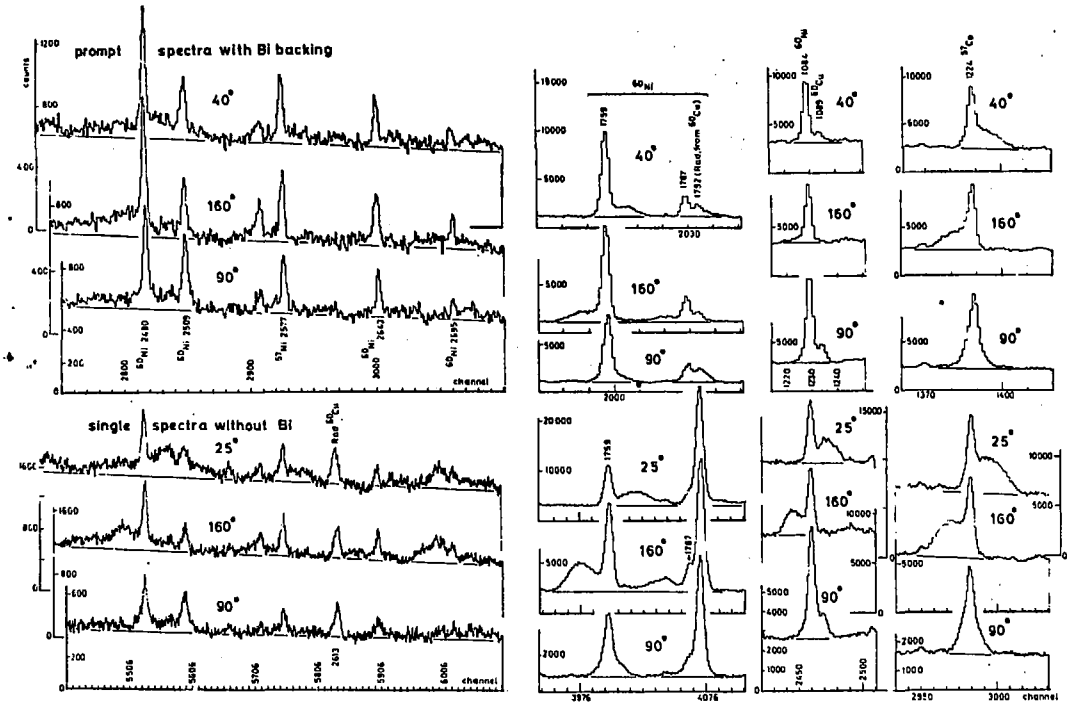
prompt spectra with Bi backing
40°
160°
90°
single spectra without Bi
25°
160°
90°
channel

Fig 6

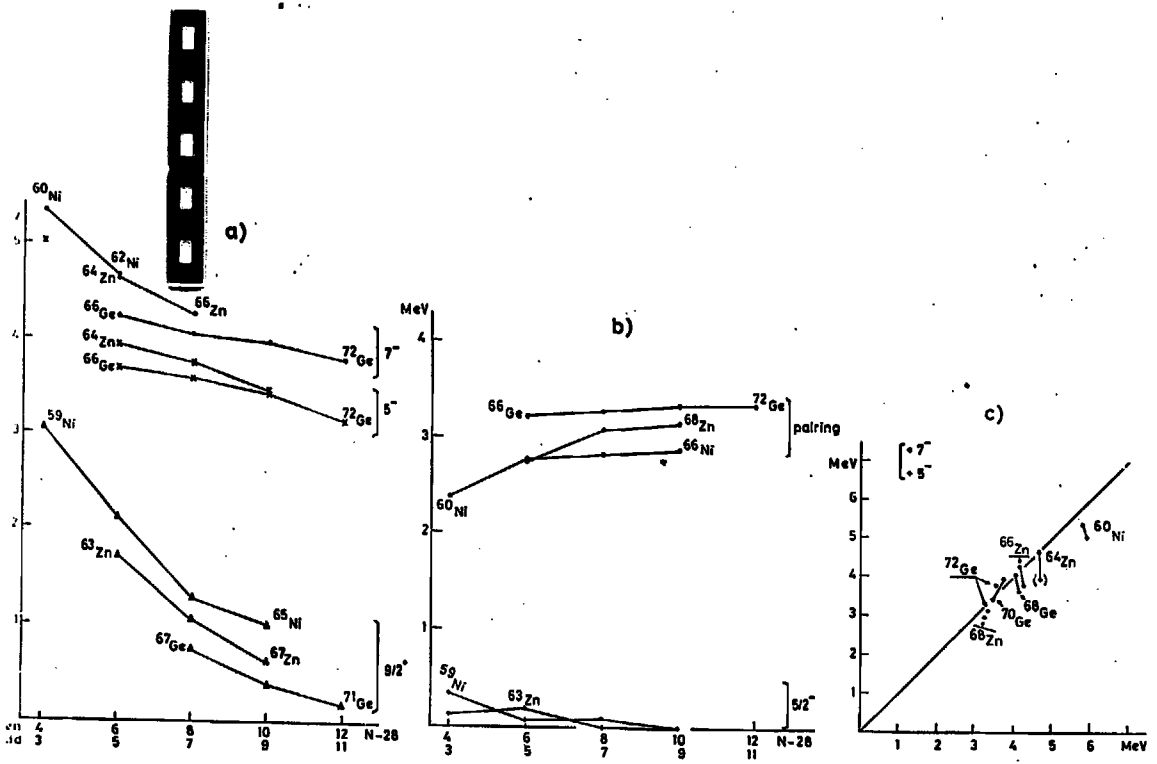
a)
^{60}Ni
^{62}Ni
^{64}Zn
^{66}Zn
^{66}Ge
^{64}Zn
^{66}Ge
^{72}Ge
7$^-$
^{72}Ge
5$^-$
^{59}Ni
^{63}Zn
^{65}Ni
^{67}Ge
^{67}Zn
^{71}Ge
9/2$^+$
N-28
MeV
b)
^{66}Ge
^{72}Ge
pairing
^{68}Zn
^{66}Ni
^{60}Ni
^{59}Ni
^{63}Zn
5/2$^-$
N-28
c)
7$^-$
5$^-$
MeV
^{60}Ni
^{66}Zn
^{64}Zn
^{72}Ge
^{70}Ge
^{68}Ge
^{68}Zn
MeV

Fig 8